ISSN 0023-1584, Kinetics and Catalysis, 2011, Vol. 52, No. 6, pp. 862–875. © Pleiades Publishing, Ltd., 2011.
Original Russian Text © P.A. Nikul'shin, A.V. Mozhaev, A.A. Pimerzin, N.N. Tomina, V.V. Konovalov, V.M. Kogan, 2011, published in Kinetika i Kataliz, 2011, Vol. 52, No. 6, pp. 884–898.

Cobalt Salts of Decamolybdodicobaltic Acid as Precursors of the Highly Reactive Type II CoMoS Phase in Hydrorefining Catalysts

P. A. Nikul'shin[a, b], A. V. Mozhaev[a], A. A. Pimerzin[a], N. N. Tomina[a], V. V. Konovalov[a], and V. M. Kogan[c]

[a] *Samara State Technical University, Samara, 443030 Russia*
[b] *Middle Volga Institute of Oil Refining, Novokuibyshevsk, Samara oblast, 446200 Russia*
[c] *Zelinsky Institute of Organic Chemistry, Russian Academy of Sciences, Moscow, 119991 Russia*
e-mail: P.A.Nikukulshin@gmail.com

Received February 7, 2011

Abstract—Catalysts have been synthesized using the Anderson polyoxometalates (POMs) $(NH_4)_4[Ni(OH)_6Mo_6O_{18}]$ ($NiMo_6POM$), $(NH_4)_6[Co_2Mo_{10}O_{38}H_4] \cdot 7H_2O$ ($Co_2Mo_{10}POM$), and $H_6[Co_2Mo_{10}O_{38}H_4]$ ($Co_2Mo_{10}HPA$) as the precursors and hydrogen peroxide as the solvent. The catalysts have been characterized by low-temperature nitrogen adsorption, XPS, and HRTEM. Their catalytic properties have been tested in thiophene hydrodesulfurization and in the hydrodesulfurization and hydrogenation of components of diesel oil. The active phase of the catalysts synthesized using the POMs is the type II CoMoS phase in which the mean plate length is 3.6–3.9 nm and the mean number of MoS_2 plate per plate packet is 1.8–2.0. Use of hydrogen peroxide provides an efficient means to reduce the proportion of Co^{2+} promoter atoms surrounded by oxygen in the case of an impregnating solution containing both an ammonium salt of a heteropoly acid and a Co^{2+} salt. In the catalysts synthesized using cobalt salts of $Co_2Mo_{10}HPA$, the support surface contains the multilayer type II CoMoS phase and cobalt sulfides. These catalyst show high catalytic properties in thiophene hydrogenolysis and diesel oil hydrorefining. Models are suggested for the catalysts synthesized using Anderson POMs.

DOI: 10.1134/S0023158411060152

The largest scale petroleum refining process is hydrorefining [1–5], and its significance will increase because of the stringent regulations imposed on the sulfur content of petroleum products in many countries. According to technical regulations adopted by the Government of the Russian Federation in 2008, the sulfur content of commercial petroleum products must be reduced by 1–2 orders of magnitude and, by 2014, the sulfur level in gasoline and diesel fuel is to be brought down to <10 ppm. The situation is aggravated by the decreasing quality of the petroleum to be refined and by the necessity of involving distillates from secondary processes in hydrorefining.

Use of new hydrorefining catalysts is among the most efficient ways of solving this problem [2–10]. It is, therefore, necessary to develop new methods for preparing highly active hydrorefining catalysts.

The active phase of supported sulfide-based hydrorefining catalysts is obtained by sulfiding an oxide precursor. The precursor is commonly synthesized from ammonium paramolybdate $(NH_4)_6Mo_7O_{24} \cdot 4H_2O$ (APM) and cobalt (nickel) nitrate. The sulfiding of the oxide precursor yields a type I Co(Ni)MoS phase, which is typically a MoS_2 monolayer chemically bonded to the support surface. Most of the Co or Ni atoms in this phase are not on MoS_2 edges, but are bound into the $Co(Ni)Al_2O_4$ spinel, which is catalytically inactive [10–12].

In recent years, new hydrorefining catalysts have been prepared by selective formation of a highly active, type II Co(Ni)MoS phase on the support surface. This phase consists of ultrafine multilayer MoS_2 packets decorated with Co (Ni) atoms [2, 4, 10]. Numerous methods have been suggested for this purpose, and they are permanently being improved [13–50]. They include use of supports varying in composition and acidity [13–24]; introduction of dopants into mixed impregnating solutions [25–31]; and use of new catalyst precursors [32–40], organic complexing agents [41–50], etc. The authors of all of these works note a marked increase in catalytic activity and explain this effect in terms of the formation of a type II CoMoS phase.

In our previous studies, we used Keggin- and Anderson-type polyoxometalates (POMs) as the precursors of hydrorefining catalysts [10, 25, 51–57] and observed that the resulting catalysts are more active in thiophene hydrodesulfurization (HDS) and in the hydrorefining of diesel oil than the catalysts prepared in the conventional way. We have found the most effi-

cient catalyst precursors [10, 51–56]: among the Anderson POMs, the most efficient one is ammonium 6-molybdonickelate $(NH_4)_4[Ni(OH)_6Mo_6O_{18}]$ (**$NiMo_6$POM**). We also reported the results of comparative tests of catalyst prepared from $NiMo_6$POM in the hydrorefining of diesel fractions with different polycyclic aromatic hydrocarbon (PAH) contents [57].

The tests of the catalysts in hydrogenation and HDS reactions demonstrated that use of $NiMo_6$POM in catalyst synthesis is favorable for the formation of a type II NiMoS phase. Application of Anderson POMs as precursors of hydrorefining catalysts was the subject of works by Cabello et al. [58–62] and by Payen and his colleagues [39, 63–65]. These authors established that the POMs decompose on being sulfided [62, 64, 65]. However, the composition of the particles on the catalyst surface remained unclear.

Pettiti et al. [62] arrived at the conclusion that the sulfiding of $CoMo_6$POM and $NiMo_6$POM produces nanostructured MoS_2 crystallites on the catalyst surface. According to EXAFS data, the promoter (Co or Ni) atoms in these catalysts are in two states, either located on MoS_2 crystallites or chemically bound into the $Co(Ni)Al_2O_4$ spinel, and it was impossible to estimate the proportions of these states.

A more detailed study was carried out on catalysts based on ammonium decamolybdodicobaltate $(NH_4)_6[Co_2Mo_{10}O_{38}H_4] \cdot 7H_2O$ (**Co_2Mo_{10}POM**) [64, 65], and it yielded somewhat different data. Lamonier et al. [65], based on EXAFS and Raman spectroscopy data, demonstrated that the decamolybdodicobaltate anion $[Co_2Mo_{10}O_{38}H_4]^{6-}$ (**Co_2Mo_{10}HPAn**) retains its structure upon drying at 100°C and calcination at 500°C. Only MoS_2 crystallites with a mean length of 2.8 nm, whose degree of packing of association species was 1.7, were observed on the surface of the sulfided catalyst. The transmission electron microscopic (TEM) images of a reference catalyst prepared from APM and cobalt nitrate showed poorly sulfided MoO_3, and this explained the low activity of this catalyst.

Mazurelle et al. [64] reported the support effect on the physicochemical and catalytic properties of Co_2Mo_{10}POM catalysts supported on Al_2O_3, TiO_2, and ZrO_2. X-ray photoelectron spectroscopy (XPS) data provided evidence that the oxide precursor (POM) turns entirely into MoS_2 upon sulfiding, and the Co2*p* binding energy indicated that the entire cobalt is in a CoMoS phase. The authors did not assign the active phase to any of its known types [11] and claimed that the nature of the support had no effect on the electronic state of Co and Mo.

Thus, the data available now do not unambiguously elucidate the type and genesis of the active phase in the catalysts synthesized using Anderson POMs. The composition of the particles on the catalyst surface is also uncertain. In particular, the location of promoter atoms on the catalyst surface is interpreted in different ways, the role of calcination in the synthesis of these catalysts is unclear, and the type of the resulting active phase is unknown. It is not fully understood why the catalysts prepared from POMs are more active more active, and the behavior of catalysts under real hydrorefining conditions remains unclear.

Here, we report the morphology of the active phase of catalysts prepared using the Anderson polyoxometalates $NiMo_6$POM and Co_2Mo_{10}POM and the acid Co_2Mo_{10}HPA, as well as the catalytic properties of the catalysts in thiophene hydrodesulfurization and in the hydrodesulfurization and hydrogenation of components of diesel oil. We also report the effect of hydrogen peroxide (POM solvent) on the composition of the particles on the support surface, on the morphology of the active phase, and on the catalytic properties.

EXPERIMENTAL

POM-Based Synthesis of Catalysts

Co_2Mo_{10}POM and $NiMo_6$POM were synthesized via procedures described in earlier works [66–69]. The synthesized POMs were identified by elemental analysis on an EDX800HS X-ray fluorescence spectrometer (Shimadzu). Their IR spectra were recorded on an Avatar 360 FTIR spectrometer (Nicolet). Raman spectra were obtained on a LabRAM spectrometer (Horiba Jobin Yvon) at $\lambda = 632.8$ nm). The phase composition of the POMs was determined by X-ray diffraction (ARLX'TRA instrument, Thermo Fisher Scientific) using CuK_α radiation. Decamolybdodicobaltic acid $H_6[Co_2Mo_{10}O_{38}H_4]$ (**Co_2Mo_{10}HPA**) was obtained from Co_2Mo_{10}POM by ion exchange in a KU-2 column [67–69].

The catalyst support was γ-Al_2O_3 with a specific surface area of 230 m^2/g and an effective pore radius of 61.9 Å. Catalysts were prepared by incipient-wetness impregnation with an aqueous solution (samples labeled with the superscript w) or a 10% hydrogen peroxide solution (samples labeled with the superscript p) of $NiMo_6$POM and $Ni(NO_3)_2 \cdot 6H_2O$ (analytical grade) or Co_2Mo_{10}POM and $Co(NO_3)_2 \cdot 6H_2O$ (reagent grade). A solution of the salt $Co_3[Co_2Mo_{10}O_{38}H_4]$ obtained by reacting of basic cobalt(II) carbonate $CoCO_3 \cdot mCo(OH)_2 \cdot nH_2O$ (reagent grade) with $H_6[Co_2Mo_{10}O_{38}H_4]$ was also used in impregnation. The reference sample was a catalyst prepared from APM (reagent grade) and cobalt nitrate $Co(NO_3)_2 \cdot 6H_2O$. The calculated Mo content of the catalysts was 10 wt %, and the calculated Co (Ni) content was 3 wt %.

The catalysts were dried in steps at 80, 100, and 120°C by holding them for 2 h at each temperature. The oxide catalysts prepared in this way were sulfided. For this purpose, a 0.25–0.50 mm size fraction of the catalyst was impregnated with the sulfiding agent di-*tert*-butyl polysulfide (54 wt % S), was placed in a glass reactor, and was sulfided with an H_2S/H_2 mixture (20 vol % H_2S) for 2 h at atmospheric pressure and $T = 400$°C.

Table 1. Characteristics of the synthesized catalysts

Catalyst	Solvent[1]	Elements contents of the catalysts, wt %			$\lambda = \frac{Co(Ni)}{Co(Ni) + Mo}$	Coke content[3], wt %	Thiophene conversion, %
		Mo	Co (Ni)	S[2]			
$Co_{3.5}$-Mo_7HPAn^p/Al_2O_3	H_2O_2	10.0	3.2	7.0	0.33	3.0	23.0
Ni_2-$NiMo_6POM^p/Al_2O_3$	H_2O_2	10.0	3.0	7.7	0.33	1.6	31.5
$Co_2Mo_{10}POM^w/Al_2O_3$	H_2O	10.0	1.2	6.3	0.16	2.8	27.2
$Co_2Mo_{10}POM^p/Al_2O_3$	H_2O_2	10.0	1.2	6.2	0.16	2.7	27.3
$Co_2Mo_{10}HPA^w/Al_2O_3$	H_2O	9.9	1.2	6.3	0.16	2.8	27.2
$Co_2Mo_{10}HPA^p/Al_2O_3$	H_2O_2	10.0	1.2	6.2	0.16	2.7	27.1
Co_3-$Co_2Mo_{10}POM^w/Al_2O_3$	H_2O	10.0	3.0	7.8	0.33	2.4	37.1
Co_3-$Co_2Mo_{10}POM^p/Al_2O_3$	H_2O_2	10.1	3.1	8.0	0.33	2.3	42.3
$Co_3[Co_2Mo_{10}HPA]^w/Al_2O_3$	H_2O	10.1	3.1	8.2	0.33	1.4	62.0
$Co_3[Co_2Mo_{10}HPA]^p/Al_2O_3$	H_2O_2	10.1	3.0	8.1	0.33	1.3	61.2

[1] The impregnating solution was prepared using water or 10% hydrogen peroxide.
[2] Sulfur content of sulfided catalysts
[3] After a 14-h-long hydrorefining test.

The metal contents of the catalysts were determined on an EDX800HS spectrometer. The sulfur content was determined before and after testing the catalysts in thiophene hydrodesulfurization in a flow reactor. The coke content of spent catalysts was also determined [70] (Table 1).

Study of the Physicochemical Properties of Catalysts

The textural characteristics of the support and catalysts were studied by low-temperature nitrogen adsorption on an Autosrb-1 adsorption porosimeter (Quantochrome). The specific surface area was calculated using the Brunauer–Emmett–Teller model for a relative partial pressure of $P/P_0 = 0.05–0.3$. The total pore volume and pore radius distribution were derived from the desorption curve using the Barrett–Joyner–Halenda model.

XPS characterization of catalysts. X-ray photoelectron spectra were recorded on a Microlab spectrometer (VG Scientific) using AlK_α radiation ($h\nu$ = 1486.6 eV) and a hemispherical electron energy analyzer. Spectra were excited with a 300-W X-ray gun. Powdered samples were secured to the holder with double-sided adhesive tape. In order to eliminate the surface charging effect, binding energy was calibrated against the O 1*s* line at 531.5 eV, which corresponded to the location of the C 1*s* line at 284.6 eV. Survey spectra were obtained at an analyzer pass energy of 100 eV. For chemical analysis and for calculation of element concentrations, some lines were recorded at a pass energy of 50 eV. X-ray Al$K_{\alpha 3,4}$ satellites were computer-subtracted from the spectral lines. The signal coaddition time ranged between a few minutes and several tens of minutes, depending on line intensity. Element concentrations on the sample surface were calculated from the C 1*s*, O 1*s*, Al 2*p*, S 2*p*, Co $2p_{3/2}$, and Mo $3p_{3/2}$ peak areas taking into account the sensitivity factors for the elements and the transmission function of the spectrometer.

The catalysts were examined by **high-resolution transmission electron microscopy (HRTEM)** on a Tecnai G2 20F microscope (FEI Company) with a LaB_6 cathode at an accelerating voltage of 200 kV and on a Tecnai G2 30F microscope with a LaB_6 cathode at an accelerating voltage of 300 kV. Catalyst samples were placed on a copper grid coated with a holey carbon film. The TEM images of all samples were obtained using a bright field technique under underfocus conditions without a lens aperture at a magnification of about ×200000. The mean MoS_2 crystallite length and the number of MoS_2 layers in the active phase packing were calculated by examining over 500 particles located in 10–15 differentv areas of the catalyst surface.

Catalytic Properties of Catalysts

The catalytic activity of catalysts in thiophene hydrogenolysis was determined using a pulsed catalytic microreactor at a hydrogen gage pressure of 0.25 atm under the following conditions: sample weight of 25 mg, 360°C, hydrogen flow rate of 20 cm^3/min, injected thiophene dose of 0.2 μl. The reaction products were separated in a quartz capillary chromatographic column with grafted OV-101 as the stationary phase.

The steady-state activity of catalyst was estimated from the thiophene conversion after 20–25 injections made at 5- to 7-min intervals. The specific catalytic activity was calculated as the amount of thiophene

Table 2. Textural characteristics of the support and those of the synthesized catalysts in oxide and sulfide forms

Catalyst	State	Specific surface area, m^2/g	Specific pore volume, cm^3/g	Mean pore diameter, Å
Al_2O_3	–	230	0.755	124
Ni_2-$NiMo_6POM^p/Al_2O_3$	Calcined	170	0.576	124
	Sulfided	155	0.554	122
$Co_2Mo_{10}HPA^w/Al_2O_3$	Calcined	190	0.596	124
	Sulfided	175	0.580	123
$Co_2Mo_{10}HPA^p/Al_2O_3$	Calcined	195	0.604	124
	Sulfided	180	0.590	123
Co_3-$Co_2Mo_{10}POM^w/Al_2O_3$	Calcined	170	0.579	124
	Sulfided	160	0.557	123
Co_3-$Co_2Mo_{10}POM^p/Al_2O_3$	Calcined	175	0.581	124
	Sulfided	160	0.538	123
$Co_3[Co_2Mo_{10}HPA]^w/Al_2O_3$	Calcined	170	0.580	124
	Sulfided	165	0.567	123
$Co_3[Co_2Mo_{10}HPA]^p/Al_2O_3$	Calcined	175	0.584	124
	Sulfided	165	0.565	123

reacted (in moles) per unit time divided by the total amount of metals in the catalyst (Mo and Co or Ni in moles): (mol C_4H_8S)(Σmol Me)$^{-1}$ s^{-1}.

Catalytic activity in the hydrorefining of diesel oil. The synthesized catalysts were tested in the hydrorefining of a mixture consisting of 20 vol % light gas oil from catalytic cracking and 80 vol % straight-run diesel oil. Both components were received from Syzranskii NPZ Co. The tests were carried out in a laboratory flow reactor. The experimental setup included temperature, pressure, and hydrogen-containing gas and liquid feed flow rate control units. The temperature in the reactor was maintained with an accuracy of ±1°C; pressure, with an accuracy of ±0.05 MPa; liquid feed flow rate, ±0.1 cm^3/h; hydrogen flow rate, ±0.2 l/h. The testing conditions were as follows: T = 320, 340, and 360°C; P = 4.0 MPa; feed LHSV of 20 h^{-1}; hydrogen : liquid feed = 600 (nl STP)/l; catalyst volume of 10 cm^3.

The hydrogenisate was sampled at 1- to 2-h intervals. The samples were treated with a 15% NaOH solution for 15 min to remove the undissolved hydrogen sulfide and were then washed with distilled water until neutral and dried with calcium chloride.

The sulfur content of the hydrogenisate was determined on an EDX800HS X-ray fluorescence analyzer. PAHs were quantified on a UV-1700 spectrophotometer (Shimadzu) [71].

The HDS activity of catalysts was estimated using the formula

$$X_{HDS} = \frac{[S]_{feed} - [S]_{hydr}}{[S]_{feed}} \times 100\%,$$

where X_{HDS} is the degree of hydrodesulfurization (%), $[S]_{feed}$ is the sulfur content of the feed (wt %), and $[S]_{hydr}$ is the sulfur content of the hydrogenisate (wt %).

The PAH hydrogenation activity of catalysts was estimated using the formula

$$X_H = \frac{[Ar]_{feed} - [Ar]_{hydr}}{[Ar]_{feed}} \times 100\%,$$

where X_H is the degree of hydrogenation of PAH (%), $[Ar]_{feed}$ is the PAH content of the feed (wt %), and $[Ar]_{hydr}$ is the PAH content of the hydrogenisate (wt %).

RESULTS AND DISCUSSION

Textural Characteristics of the Catalysts

The compositions of the synthesized catalysts are listed in Table 1. The catalysts differ in Co (Ni) : Mo molar ratio (λ). For the samples synthesized from $Co_2Mo_{10}POM$ or $Co_2Mo_{10}HPA$, the molar ratio of the metals is initially determined by the molecular formula of the polyoxometalate anion; that is, Co : Mo = 1 : 5, or λ = 0.16. The catalysts with λ = 0.33 were additionally promoted with cobalt. The sulfur content of the sulfided catalysts ranges between 6.2 and 8.2 wt % (Table 1), indicating that the metals are sulfided to a large extent.

Loading of the initial support γ-Al_2O_3 with an oxide precursor decreases its specific surface area and specific pore volume by 15–30% (Table 2). In order to study the structure of the supported polyoxometalates, we recorded the IR spectra of the catalysts in oxide form (Fig. 1). The spectra show absorption bands characteristic of $Co_2Mo_{10}HPAn$, indicating that the structure of the polyoxometalate anion is unchanged

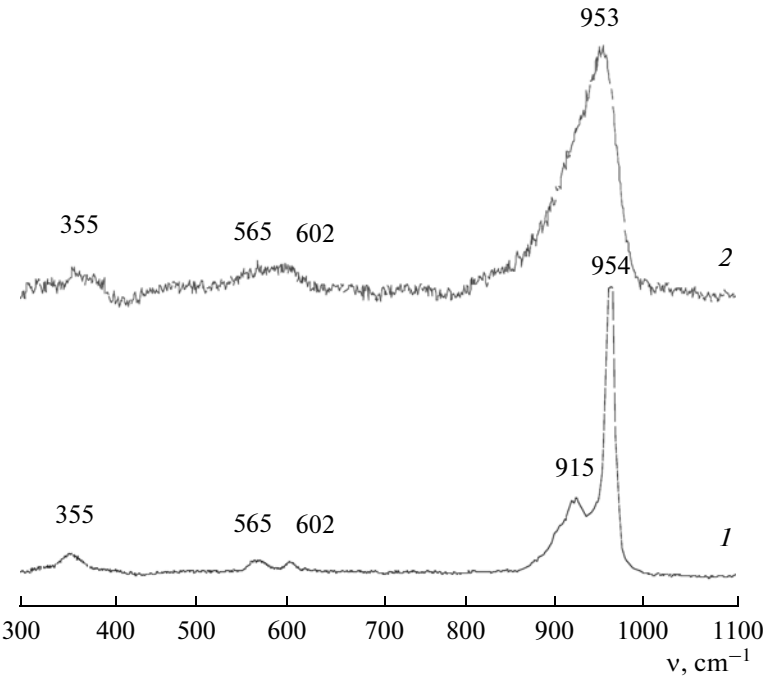

Fig. 1. Raman spectra of (*1*) $Co_2Mo_{10}POM$ and (*2*) Co_3-$Co_2Mo_{10}POM^p/Al_2O_3$ dries at 120°C.

after the impregnation and drying stages. This fact is in agreement with the earlier reports that the polyoxometalate structure survives the impregnation and drying stages [63, 64].

The deposition of an active precursor and subsequent sulfiding exert no significant effect on the effective pore diameter of the samples; therefore, the active phase forms in mesopores of the support (Fig. 2). The sulfiding of the oxide samples causes a slight decrease in their specific surface area and specific pore volume because of the change in the morphology of the supported polyoxometalates and their conversion into the active sulfide phase. These changes are independent of the catalyst preparation procedure (composition of the impregnating solution).

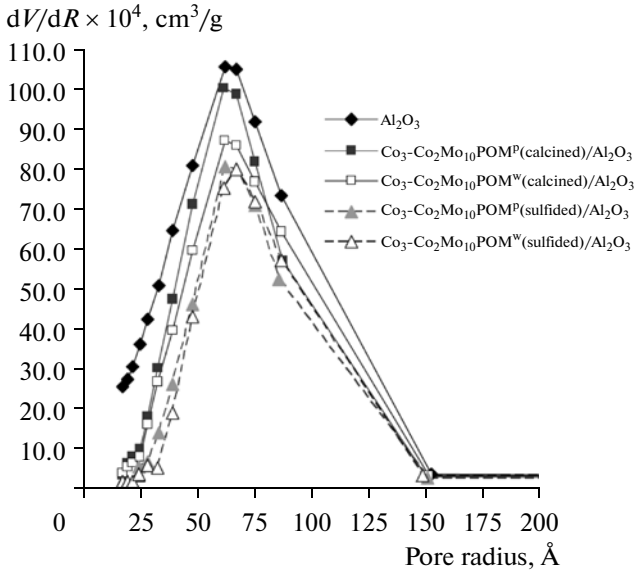

Fig. 2. Pore radius distribution in the support and in the Co_3-$Co_2Mo_{10}POM^p/Al_2O_3$ and Co_3-$Co_2Mo_{10}POM^w/Al_2O_3$ catalysts in oxide (calcined) and sulfided forms.

Properties of the Active Phase of the Catalysts

XPS data provided detailed information concerning the active sulfide phase of the synthesized catalysts (Fig. 3). The Mo 3*d* profiles of the sulfided catalysts are well-resolved doublets occurring at a binding energy of BE(Mo $3d_{5/2}$) = 229.0 eV, which is characteristic of MoS_2 [72–76]. The peak at BE = 235.2 eV, which would be characteristic of molybdenum (Mo^{5+} and/or Mo^{6+}) in an oxide environment (molybdenum oxide or oxysulfide), is practically absent. This is evidence that $Co_2Mo_{10}HPAn$ is entirely sulfided. The state of the Mo atoms in the sulfide catalysts is independent of the composition of the impregnating solution.

The Co 2*p* spectra of the sulfide catalysts suggest that cobalt in these catalysts is in different types of environments. The sulfiding of the catalysts synthesized from $Co_2Mo_{10}HPAn$ alone without introducing an extra amount of a promoter ($Co_2Mo_{10}POM^p/Al_2O_3$, $Co_2Mo_{10}HPA^p/Al_2O_3$) results in the total sulfiding of the promoter atoms located inside $Co_2Mo_{10}HPAn$. The XPS spectrum of the sulfided product shows only

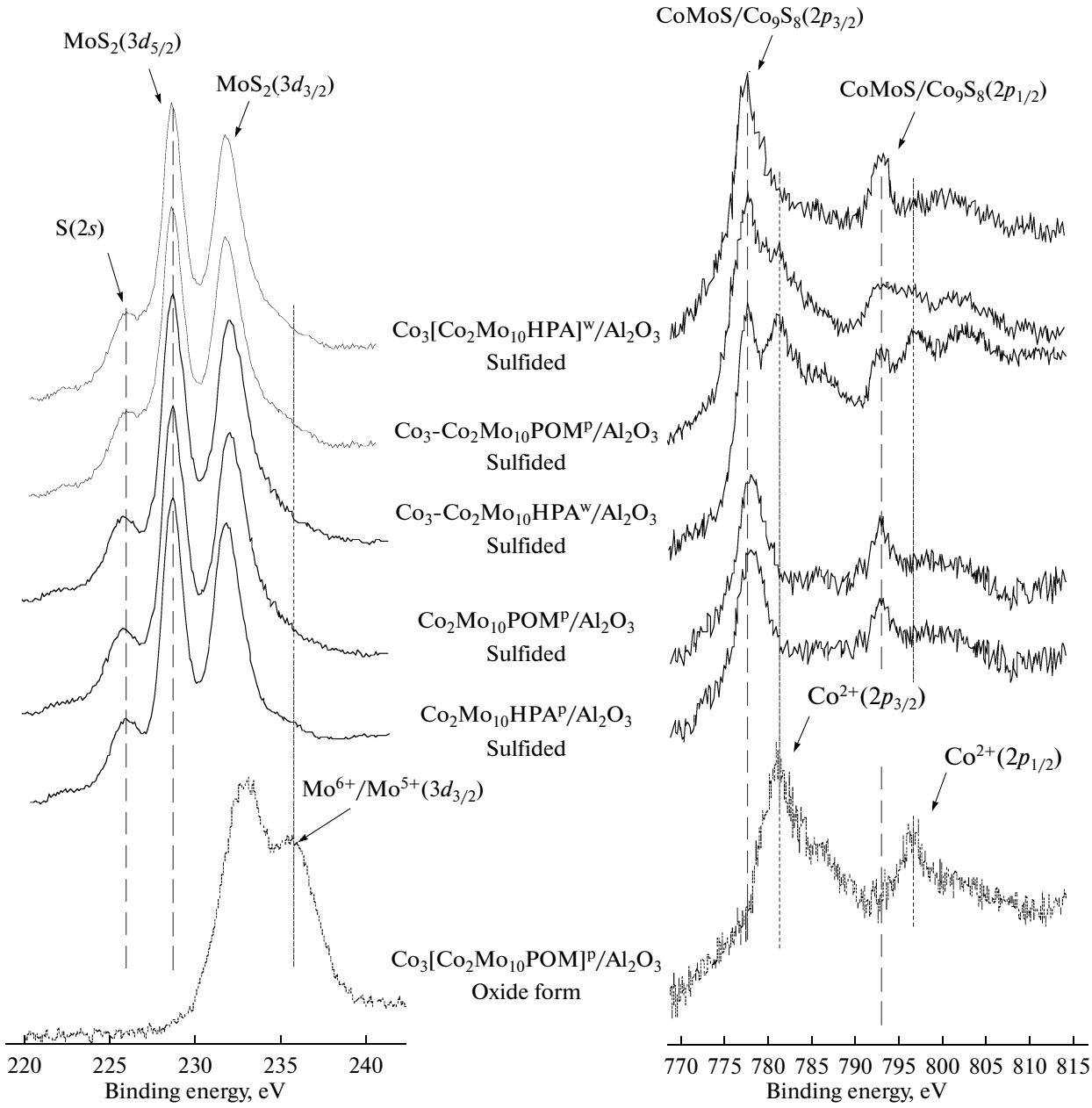

Fig. 3. X-ray photoelectron spectra (Mo 3*d* and Co 2*p* lines) of the $Co_2Mo_{10}POM^p/Al_2O_3$, $Co_2Mo_{10}HPA^p/Al_2O_3$, Co_3-$Co_2Mo_{10}POM^p/Al_2O_3$, and $Co_3[Co_2Mo_{10}HPA]^p/Al_2O_3$ in oxide and sulfided forms.

a peak at BE = 779.0 eV, which is characteristic of Co $2p_{3/2}$ in a sulfide environment [75–81]. According to Alstrup et al. [77], the CoMoS phase is identified as the difference between the Co $2p_{3/2}$, Mo $3d_{5/2}$, and S $2p$ binding energies. For the catalysts examined, BE(Co $2p_{3/2}$) – BE(Mo $3d_{5/2}$) = 550 ± 0.2 eV and BE(Co $2p_{3/2}$) – BE(S $2p$) = 617 ± 0.2 eV, which is evidence in favor of the formation of the CoMoS phase. This is likely due to the short distance between the Mo and Co atoms (both in the same polyoxometallate anion), which makes possible the complete sulfiding of both metals.

Promotion of the catalysts with an extra amount of cobalt introduced as cobalt nitrate into the mixed impregnating solution at the impregnation stage changes the XPS spectrum. For the Co_3-$Co_2Mo_{10}POM^w/Al_2O_3$ sample, the spectrum shows, along with the main peak at BE = 779.0 eV, a peak at BE = 782.2 eV, which is characteristic of Co^{2+} in an oxygen environment [78, 80, 81]. Thus, the promotion of the catalyst with an additional amount of cobalt causes the formation of both sulfide and oxide particles on the surface. Use of hydrogen peroxide solution at the catalyst synthesis stage leads to a weakening of the peak due to Co^{2+} in

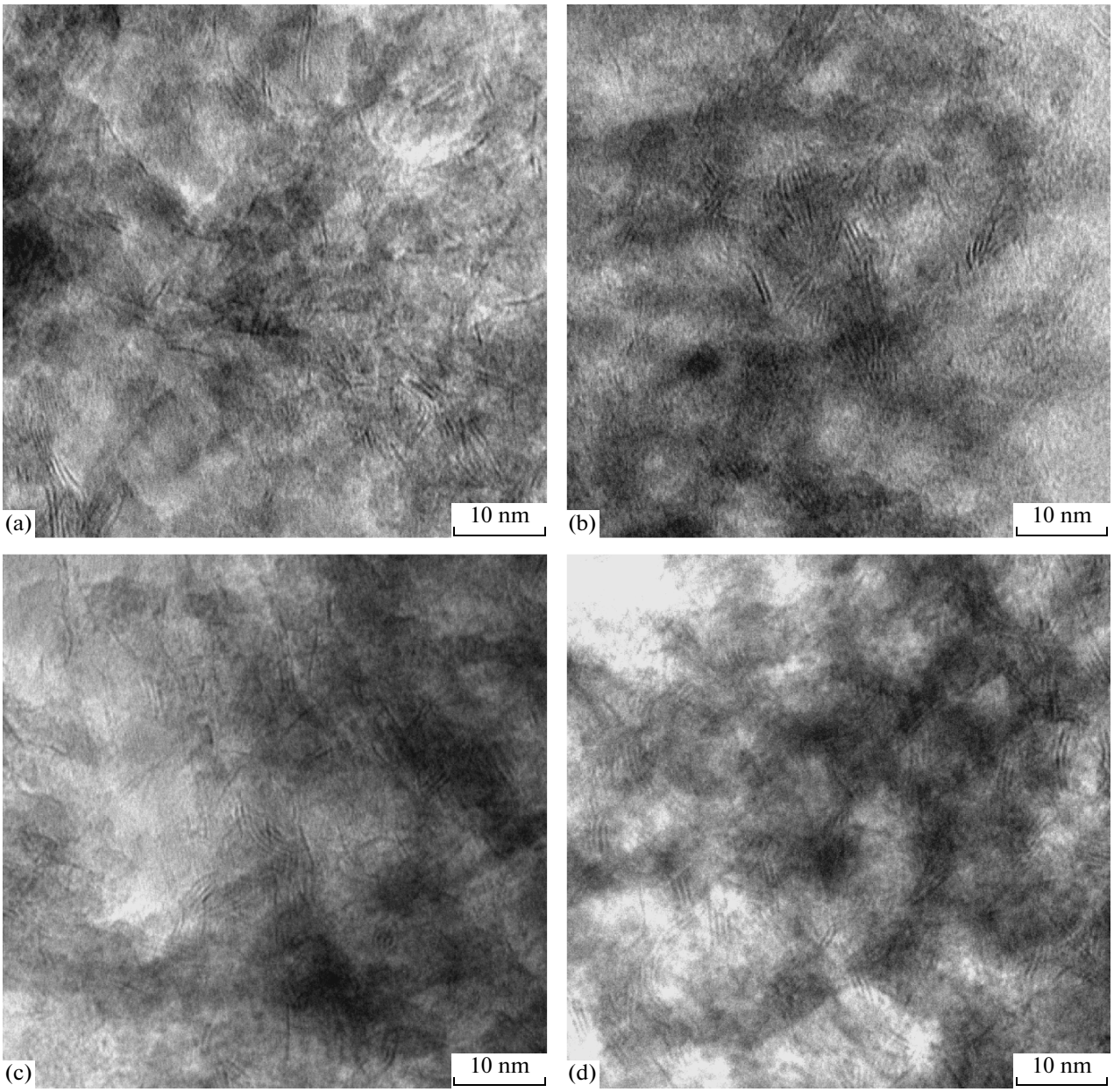

Fig. 4. TEM images of sulfide catalyst samples: (a) Ni_2-$NiMo_6POM^p/Al_2O_3$, (b) $Co_2Mo_{10}HPA^w/Al_2O_3$, (c) Co_3-$Co_2Mo_{10}{}^p/Al_2O_3$, and (d) $Co_3[Co_2Mo_{10}HPA]^w/Al_2O_3$.

an oxygen environment; therefore, a larger proportion of cobalt undergoes sulfiding. Use of the cobalt salt of $Co_2Mo_{10}HPA$ yields a catalyst in which the promoter atoms are entirely sulfided ($Co_3[Co_2Mo_{10}HPA^w/Al_2O_3$ sample).

The TEM images of the synthesized catalysts are presented in Fig. 4. The mean values of the active phase crystallite length and of the number of plates in a MoS_2 association species are listed in Table 3. The active phase of the catalysts is type II CoMoS, and its particle consists of several MoS_2 plates with a mean length of 3.6–3.9 nm. The mean number of MoS_2 plates in an association species is 1.8–2.0. The active phase of the catalysts synthesized using $Co_2Mo_{10}HPAn$ has a larger number of MoS_2 plates than the sample synthesized from $NiMo_6POM$. The catalysts promoted with an extra amount of cobalt have a larger number of MoS_2 plates per packet than the catalysts prepared using $Co_2Mo_{10}HPA$ (Table 3). Use of hydrogen peroxide as a component of the mixed impregnating solution does not produce any significant effect on the morphology of the active phase of the catalysts.

Table 3. Geometric parameters of the nanostructures active phase of the sulfide-based hydrorefining catalysts synthesized using Anderson POMs

Catalyst	Mean length of active component particles	Mean number of MoS_2 plates per active component packet
Ni_2-$NiMo_6POM^w/Al_2O_3$	3.8	1.8
$Co_2Mo_{10}HPA^w/Al_2O_3$	3.8	1.8
Co_3-$Co_2Mo_{10}POM^p/Al_2O_3$	3.9	2.0
$Co_3[Co_2Mo_{10}HPA]^w/Al_2O_3$	3.8	2.0
$Co_3[Co_2Mo_{10}HPA]^p/Al_2O_3$	3.8	2.0

Catalytic Properties of the Synthesized Catalysts

The thiophene HDS activity data for the catalysts are presented in Table 1 and Fig. 5. The thiophene conversion in the catalytic tests was 23–62%. The lowest thiophene conversion (23.0%) was observed for the reference sample, which was synthesized using APM (Table 1). The highest thiophene conversion (61.2–62.0%) was attained with the catalysts based on the cobalt salts of $Co_2Mo_{10}HPA$.

The highest specific catalytic activity in thiophene HDS are again shown by the samples based on the cobalt salts of $Co_2Mo_{10}HPA$. The catalyst based on $Co_2Mo_{10}POM$ ($Co_2Mo_{10}POM^w/Al_2O_3$) with a lower promoter content has a higher specific catalytic activity than the sample synthesized using $NiMo_6POM$ with the optimum Ni : Mo ratio ($\lambda = 0.33$). Use of a hydrogen peroxide solution as the solvent exerts no effect on the specific thiophene HDS activity of the catalysts prepared using $Co_2Mo_{10}HPAn$ alone. In the case of the additionally promoted catalytic systems based on $Co_2Mo_{10}POM$, use of H_2O_2 at the impregnating solution preparation stage raises the specific catalytic activity by ~15% (compare Co_3-$Co_2Mo_{10}POM^w/Al_2O_3$ and Co_3-$Co_2Mo_{10}POM^p/Al_2O_3$). Use of cobalt salts enhances the specific catalytic activity even more greatly (by a factor of 1.7). Use of hydrogen peroxide in the synthesis of the catalysts based on the cobalt salts of $Co_2Mo_{10}HPA$ does not change the specific catalytic activity in thiophene HDS.

In the hydrorefining of real feedstocks, the catalysts prepared using $Co_2Mo_{10}HPAn$ show a higher HDS activity than Ni_2-$NiMo_6POM^p/Al_2O_3$ (Fig. 6). However, the hydrogenation activity of the Ni_2-$NiMo_6POM^p/Al_2O_3$ catalyst than that of the catalysts based on $Co_2Mo_{10}HPAn$. The introduction of hydrogen peroxide into the impregnating solution produces no effect on the catalytic properties of the catalysts synthesized using $Co_2Mo_{10}POM$ or $Co_2Mo_{10}HPA$.

Promotion of the $Co_2Mo_{10}POM$-based catalysts with an extra amount of cobalt enhances their HDS and hydrogenation activities (Fig. 7). Use of hydrogen peroxide also improves the catalytic properties. The highest HDS and hydrogenation activities are shown by the catalysts obtained using the cobalt salts of $Co_2Mo_{10}HPA$; however, the hydrogen peroxide solution used as the solvent does not change the catalytic activity of these catalysts.

The coke forming on the catalyst surface during hydrorefining blocks active sites and is among the causes of the decrease in catalytic activity. The operating stability of the catalysts can be indirectly evaluated in terms of the amount of coke on their surface. an analysis of coke content data for spent catalysts (Table 1) suggests that the least stable performance is shown by the samples synthesized using APM and $Co_2Mo_{10}POM$ (their coke content is 2.8–3.0 wt %). The smallest amount of coke after catalytic tests (1.3–1.6 wt %) is observed for Ni_2-$NiMo_6POM^p/Al_2O_3$, $Co_3[Co_2Mo_{10}HPA]^w/Al_2O_3$, and $Co_3[Co_2Mo_{10}HPA]^p/Al_2O_3$.

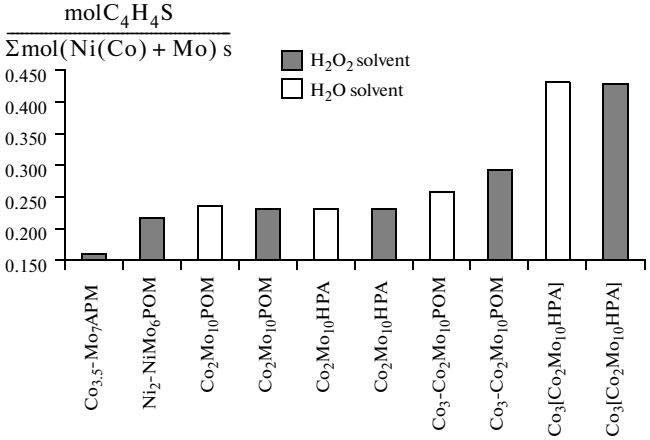

Fig. 5. Comparison of the specific catalytic activities of catalysts synthesized using Anderson POMs and APM in thiophene hydrogenolysis.

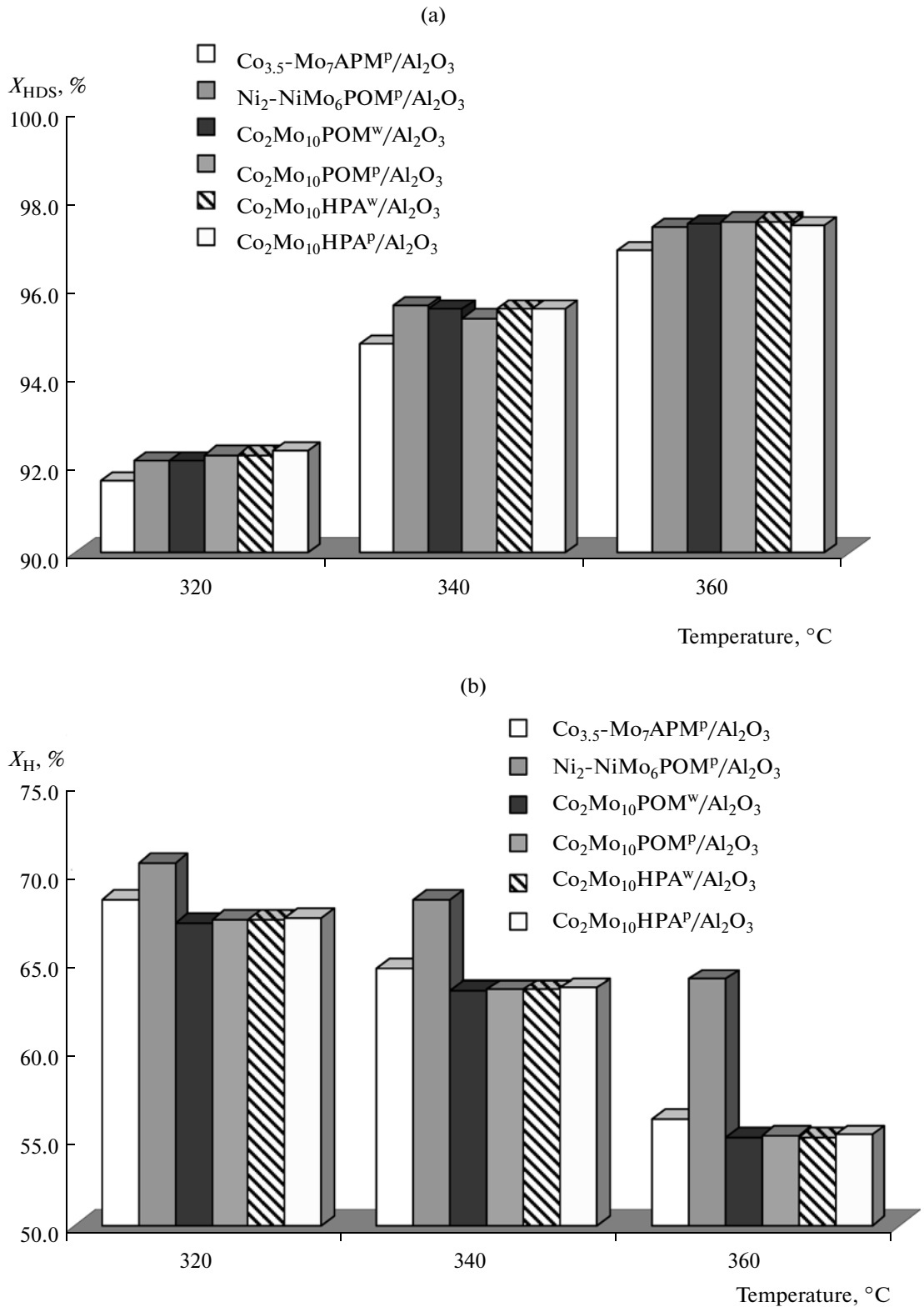

Fig. 6. (a) HDS and (b) hydrogenation activities of catalysts synthesized using APM, $NiMo_6POM$, and $Co_2Mo_{10}POM$ in diesel oil hydrorefining at 320–360°C. $P = 4.0$ MPa, LHSV = 2 h^{-1}, hydrogen-containing gas : liquid feed = 600 (l STP)/l.

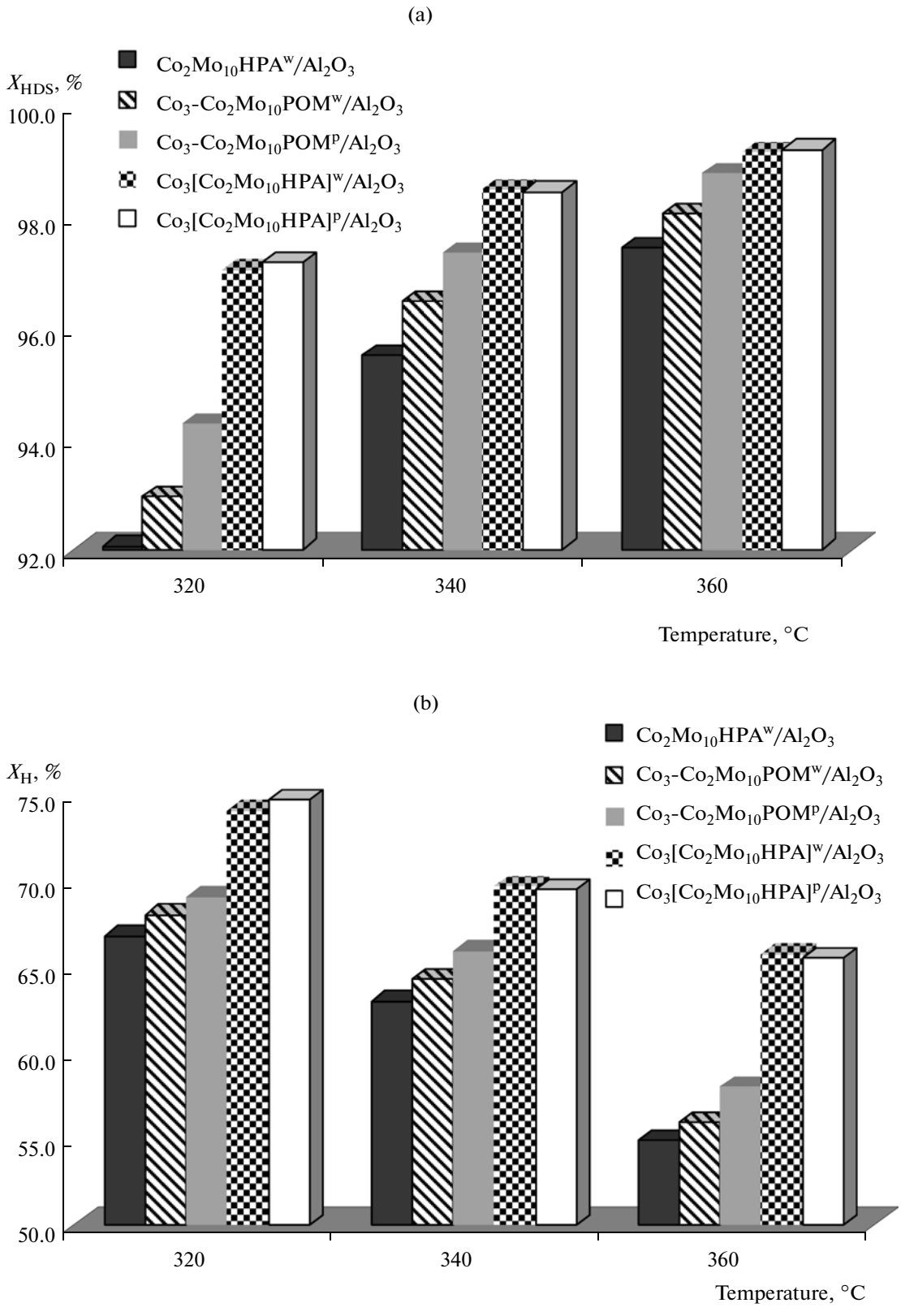

Fig. 7. (a) HDS and (b) hydrogenation activities of catalysts synthesized using Co_2Mo_{10}POM Co_2Mo_{10}HPA and in diesel oil hydrorefining at 320–360°C. $P = 4.0$ MPa, LHSV = 2 h^{-1}, hydrogen-containing gas : liquid feed = 600 (l STP)/l.

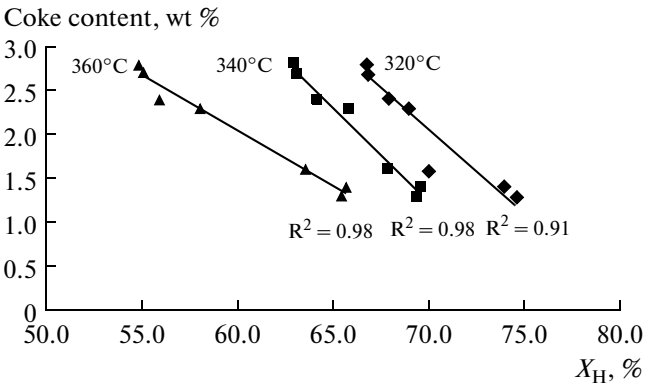

Fig. 8. Coke content of spent catalysts tested in diesel oil hydrorefining at 320–360°C versus their hydrogenation activity.

The coke content of the spent catalysts correlates well with their hydrogenation activity (Fig. 8). This can be explained by the fact that the coke precursors are extremely unsaturated polycyclic naphthenes and condensed aromatic hydrocarbons. The higher the hydrogenation activity of a catalyst, the higher its hydrogenation activity toward coke precursors and, accordingly, the lower the coke content of the catalyst.

An analysis of the composition and structure of the active phase of the catalysts prepared using Co_2Mo_{10}HPAn from different impregnating solutions at different synthesis stages suggests the active phase structure model presented in Fig. 9.

Based on the fact that the active phase has a hexagonal structure, taking the approaches developed in earlier works [49, 82], it is possible to estimate the proportion of molybdenum atoms located on the edges of the MoS_2 crystallites. For the known geometric char-

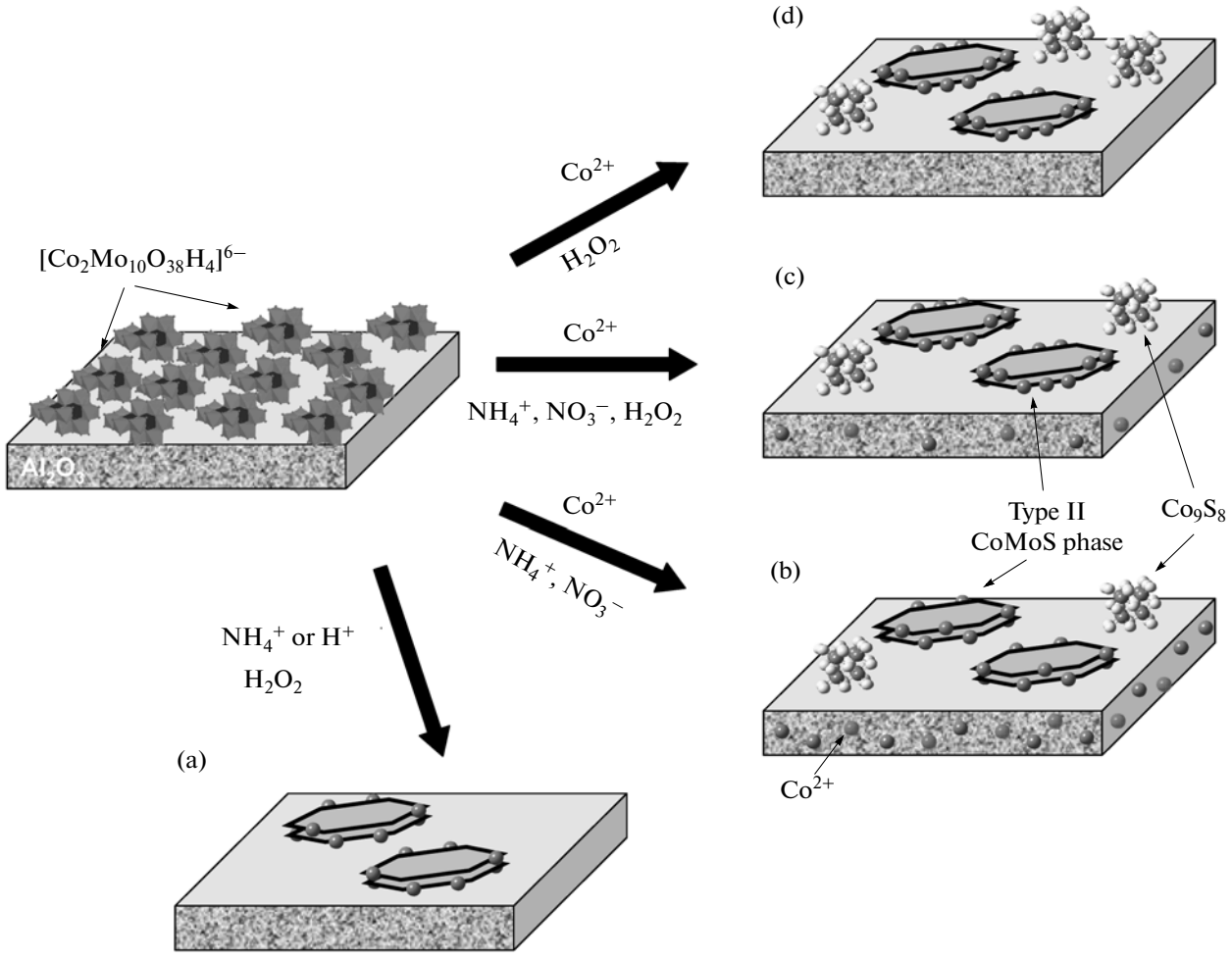

Fig. 9. Models of sulfided catalysts prepared using Co_2Mo_{10}POM: (a) $Co_2Mo_{10}POM^w/Al_2O_3$ or $Co_2Mo_{10}HPA^w/Al_2O_3$, (b) Co_3-$Co_2Mo_{10}POM^w/Al_2O_3$, (c) Co_3-$Co_2Mo_{10}POM^p/Al_2O_3$, and (d) $Co_3[Co_2Mo_{10}HPA]^w/Al_2O_3$.

acteristics of the active phase (mean crystallite length, 3.6–3.9 nm; mean number of MoS_2 plates per packet, 1.8–2.0), the edges of the active phase crystallites can accommodate 30–32% of the total number of molybdenum atoms. Thus, provided that the MoS_2 edges are completely occupied and each edge molybdenum atom binds one cobalt atom, the theoretical fraction of promoter atoms that can be accommodated by the active phase is ~0.3. At Co : Mo = 0.2 mol/mol for catalysts based on only Co_2Mo_{10}POM and Co_2Mo_{10}HPA, 20% of the cobalt atoms (relative to the total n umber of molybdenum atoms) can theoretically be located on the edges of molybdenum sulfide crystallites. Because of this, use of Co_2Mo_{10}POM or Co_2Mo_{10}HPA in catalyst synthesis leads to the formation of a multilayer, promoter-deficient, type II CoMoS phase (Fig. 9a). Use of hydrogen peroxide as the solvent produces no effect on the composition and morphology of the active phase (Fig. 3) and catalytic properties (Figs. 5, 6).

The Co_3-$Co_2Mo_{10}POM^w/Al_2O_3$ catalyst (Fig. 9b), promoted with an extra amount of cobalt up to Co : Mo = 0.5 in the presence of ammonium cations and nitrate anions, also contains the promoter-deficient type II CoMoS phase. (XPS data (Fig. 3) indicate the presence of cobalt in an oxygen environment.) According to XPS data, use of hydrogen peroxide as the solvent (Fig. 9c) decreases the number of promoter atoms in an oxygen environment (Fig. 3), and this effect shows itself as an increase in the catalytic activity both in thiophene HDS and in diesel oil hydrorefining (Figs. 5, 7). The model of the catalyst synthesized using the cobalt salt of Co_2Mo_{10}HPA is the type II CoMoS phase with completely occupied MoS_2 edges and Co_9S_8 particles (Fig. 9d). Use of the hydrogen peroxide solution as the solvent in the synthesis of $Co_3[Co_2Mo_{10}HPA]^p/Al_2O_3$ produces no effect on the composition of the particles on the support surface, as in the case of $Co_2Mo_{10}POM^w/Al_2O_3$ and $Co_2Mo_{10}POM^p/Al_2O_3$ ($Co_2Mo_{10}HPA^w/Al_2O_3$ and $Co_2Mo_{10}HPA^p/Al_2O_3$). Thus, use of hydrogen peroxide provides an efficient means to reduce the proportion of the Co^{2+} promoter atoms surrounded by oxygen in the case of an impregnating solution containing both an ammonium salt of a heteropoly acid and a cobalt salt. The role of hydrogen peroxide is likely to oxidize part of the ammonium cations and to produce peroxo polyoxometalates, which are more soluble than the ammonium salts of the heteropoly acids. This leads to the partial formation of the cobalt salts of Co_2Mo_{10}HPA. This is the reason why the activity of Co_3-$Co_2Mo_{10}POM^p/Al_2O_3$ is intermediate between the activities of Co_3-$Co_2Mo_{10}POM^w/Al_2O_3$ and $Co_3[Co_2Mo_{10}HPA]^w/Al_2O_3$ (Figs. 5, 7). Because the impregnating solution used in the synthesis of catalysts from only Co_2Mo_{10}HPAn ($Co_2Mo_{10}POM^w/Al_2O_3$ and $Co_2Mo_{10}HPA^w/Al_2O_3$) contains no cobalt cations, hydrogen peroxide exerts no effect on the composition of the particles on the support surface and on the catalytic properties. In the synthesis of catalysts based on the cobalt salts of Co_2Mo_{10}HPA ($Co_3[Co_2Mo_{10}HPA]^w/Al_2O_3$), hydrogen peroxide again produces no effect, because the mixed impregnating solution contains no ammonium ions.

CONCLUSIONS

The active phase of the catalysts synthesized using $NiMo_6$POM, Co_2Mo_{10}POM, and Co_2Mo_{10}HPA is the type II CoMoS phase with a mean plate length of 3.60–3.85 nm and 1.76–4.98 plates per packet.

Use of hydrogen peroxide is an efficient means to reduce the proportion of promoter (Co^{2+}) atoms surrounded by oxygen in the case of an impregnating solution containing both an ammonium salt of a heteropoly acid and a $^{2+}$ salt.

The catalysts synthesized using the cobalt salts of Co_2Mo_{10}HPA contain a multilayer type II CoMoS phase and cobalt sulfides on their surface and show high catalytic activity in thiophene hydrogenolysis and in diesel oil hydrorefining.

Models are suggested for catalysts synthesized using Anderson POMs.

ACKNOWLEDGMENTS

This work was carried out in the framework of the federal target program "Research and Pedagogical Cadre for Innovative Russia" for 2009–2013. A.V. Mozhaev is grateful to Haldor Topsøe Co. for a dissertation grant.

REFERENCES

1. Levinbuk, M.I., Netesanov, S.D., Lebedev, A.A., Borodacheva, A.V., and Sizova, E.V., *Pet. Chem.*, 2007, vol. 47, no. 4, p. 230.
2. Parlevliet, F. and Eijsbouts, S., *Catal. Today*, 2008.
3. Duplyakin, V.K., *Ros. Khim. Zh.*, 2008, vol. 51, no. 4, p. 11.
4. Song, Ch., *Catal. Today*, 2003, vol. 86, p. 211.
5. Babich, I.V. and Moulijn, J.A., *Fuel*, 2003, vol. 82, p. 607.
6. Nefedov, B.K., *Katal. v Prom–sti,* 2003, vol. 2, p. 20.
7. Startsev, A.N., *Sul'fidnye katalizatory gidroochistki: sintez, struktura, svoistva* (Sulfide Catalysts for Hydrorefining: Synthesis, Structure, and Properties), Novosibirsk: Geo, 2008.
8. Kogan, V.M., *Doctoral (Chem.) Dissertation*, Moscow: Inst. of Organic Chemistry, 2005.
9. Leliveld, R.G. and Eijsbouts, S.E., *Catal. Today*, 2008, vol. 130, p. 183.
10. Tomina, N.N., Pimerzin, A.A., and Moiseev, I.K., *Ros. Khim. Zh.*, 2008, vol. 52, no. 4, p. 41.
11. Topsøe, H., Clausen, B.S., and Massoth, F.E., *Hydrotreating Catalysis Science and Technology*, New York: Springer, 1996.
12. Topsøe, H., *Appl. Catal., A*, 2007, vol. 322, p. 3.

13. Usman, U., Takaki, M., Kubota, T., and Okamoto, Y., *Appl. Catal., A*, 2005, vol. 286, p. 148.
14. Usman, U., Kubota, T., Araki, Y., Ishida, K., and Okamoto, Y., *J. Catal.*, 2004, vol. 227, p. 523.
15. Usman, T., Kubota, I., and Hiromitsu, Y., *J. Catal.*, 2007, vol. 247, p. 78.
16. Dumeignil, F., Sato, K., Imamura, M., Matsubayashi, N., Payen, E., and Shimada, H., *Appl. Catal., A*, 2006, vol. 315, p. 18.
17. Giraldo, S.A. and Centeno, A., *Catal. Today*, 2008, vol. 255, p. 133.
18. Maity, S.K., Flores, G.A., Ancheyta, J., and Rana, M.S., *Catal. Today*, 2008, vol. 130, p. 374.
19. Ding, L., Zhang, Z., Zheng, Y., Ring, Z., and Chen, J., *Appl. Catal., A*, 2006, vol. 301, p. 241.
20. Kim, H., Lee, J.J., and Moon, S.H., *Appl. Catal., B*, 2003, vol. 44, p. 287.
21. Mey, D., Brunet, S., Canaff, C., Mauge, F., Bouchy, C., and Diehl, F., *J. Catal.*, 2004, vol. 227, p. 436.
22. Fan, Y., Lu, J., Shi, G., Liu, H., and Bao, X., *Catal. Today*, 2007, vol. 125, p. 220.
23. Mizutani, H., Godo, H., Ohsaki, T., Kato, Y., Fujikawa, T., Saih, Y., Funamoto, T., and Segawa, K., *Appl. Catal., A*, 2005, vol. 295, p. 193.
24. Li, X., Wang, A., Zhang, S., Chen, Y., and Hu, Y., *Appl. Catal., A*, 2007, vol. 316, p. 134.
25. Tomina, N.N., Pimerzin, A.A., Loginova, A.N., Sharikhina, M.A., Zhilkina, E.O., and Eremina, Yu.V., *Pet. Chem.,* 2004, vol. 44, no. 4, p. 246.
26. Hubaut, R., *Appl. Catal., A*, 2007, vol. 322, p. 121.
27. Ho, T.C., *Catal. Today*, 2008, vol. 130, p. 206.
28. Ho, T.C., *Catal. Today,* 2004, vol. 98, p. 3.
29. Linares, C.F. and Fernandez, M., *Catal. Lett.*, 2008, vol. 126, p. 341.
30. Ferdous, D., Dalai, A.K., Adjaye, J., and Kotlyar, L., *Appl. Catal., A*, 2005, vol. 294, p. 80.
31. Spojakina, A.A., Kraleva, E.U., and Jiratova, K., *Bulg. Chem. Commun.*, 2002, vol. 34, no. 3.
32. Breysse, M., Geantet, C., Afanasiev, P., Blanchard, J., and Vrinat, M., *Catal. Today*, 2008, vol. 130, p. 3.
33. Kraleva, E., Spojakina, A., Jiratova, K., and Petrov, L., *Catal. Lett.*, 2006, vol. 112, p. 203.
34. Spojakina, A., Kraleva, E., Jiratova, K., and Petrov, L., *Appl. Catal., A*, 2005, vol. 288, p. 10.
35. Spojakina, A., Jiratova, K., Kostova, N., Kocianova, J., and Stamenova, M., *Kinet. Catal.*, 2003, vol. 44, no. 6, p. 813.
36. Palcheva, R., Spojakina, A., Tyuliev, G., Jiratova, K., and Petrov, L., *Kinet. Catal.*, vol. 48, p. 847.
37. Shafi, R., Siddiqui, M.R.H., Hutchings, G.J., Derouane, E.G., and Kozhevnikov, I.V., *Appl. Catal., A*, 2000, vol. 204, p. 251.
38. Pawelec, B., Mariscal, R., Fierro, J.L.G., Greenwood, A., and Vasudevan, P.T., *Appl. Catal., A,* 2001, vol. 206, p. 295.
39. Blanchard, P., Lamonier, C., Griboval, A., and Payen, E., *Appl. Catal., A*, 2007, vol. 322, p. 33.
40. Lizama, L. and Klimova, T., *Appl. Catal., B,* 2008, vol. 82, p. 139.
41. Kishan, G., Coulier, L., Veen, J.A.R., and Niemantsverdriet, J.W., *J. Catal.*, 2001, vol. 200, p. 194.
42. Kishan, G., Coulier, L., Veen, J.A.R., and Niemantsverdriet, J.W., *J. Catal.*, 2000, vol. 196, p. 189.
43. Coulier, L., Beer, V.H.J., Veen, J.A.R., and Niemantsverdriet, J.W., *J. Catal.*, 2001, vol. 197, p. 26.
44. Al-Dalama, K., Aravind, B., and Stanislaus, A., *Appl. Catal., A*, 2005, vol. 296, p. 49.
45. Okamoto, Y., Ishihara, Sh., Kawano, M., Satoh, M., and Kubota, T., *J. Catal.*, 2003, vol. 217, p. 12.
46. Mazoyer, P., Geantet, C., Diehl, F., Loridant, S., and Lacroix, M., *Catal. Today*, 2008, vol. 130, p. 75.
47. Rana, M.S., Ramirez, J., Gutierrez-Alejandre, A., Ancheyta, J., Cedeno, L., and Maity, S.K., *J. Catal.*, 2007, vol. 246, p. 100.
48. Lelias, M.A., van Gestel, J., Mauge, F., and van Veen, J.A.R., *Catal. Today*, 2008, vol. 130, p. 109.
49. Hensen, E.J.M., Kooyman, P.J., van der Meer, Y., van der Kraan, A.M., de Beer, V.H.J., van Veen, J.A.R., and van Santen, R.A., *J. Catal.*, 2001, vol. 199, p. 224.
50. Hensen, E.J.M., van der Kraan, A.M., de Beer, V.H.J., van Veen, J.A.R., and van Santen, R.A., *Catal. Lett.*, 2002, vol. 84, p. 59.
51. Nikul'shin, P.A., Eremina, Yu.V., Tomina, N.N., and Pimerzin, A.A., *Pet. Chem.*, 2006, vol. 46, p. 343.
52. Nikul'shin, P.A., Tomina, N.N., and Pimerzin, A.A., *Izv. Vyssh. Uchebn. Zaved., Khim. Khim. Tekhnol.*, 2007, vol. 50, no. 9, p. 54.
53. Nikul'shin, P.A., Tomina, N.N., Ishutenko, D.I., and Pimerzin, A.A., *Izv. Vyssh. Uchebn. Zaved., Khim. Khim. Tekhnol.*, 2008, vol. 51, no. 9, p. 51.
54. Tomina, N.N., Nikul'shin, P.A., and Pimerzin, A.A., *Pet. Chem.*, 2008, vol. 48, no. 2, p. 92.
55. Tomina, N.N., Nikul'shin, P.A., and Pimerzin, A.A., *Kinet. Catal.*, 2008, vol. 49, no. 5, p. 653.
56. Tomina, N.N., Nikul'shin, P.A., Tsvetkov, V.S., and Pimerzin, A.A., *Kinet. Catal.*, 2009, vol. 50, no. 2, p. 220.
57. Nikul'shin, P.A., Tomina, N.N., Eremina, Yu.V., and Pimerzin, A.A., *Russ. J. Appl, Chem.*, 2009, vol. 82, no. 1, p. 86.
58. Cabello, C.I., Munoz, M., Payen, E., and Thomas, H.J., *Catal. Lett.*, 2004, vol. 92, p. 69.
59. Cabello, C.I., Cabrerizo, F.M., Alvarez, A., and Thomas, H.J., *J. Mol. Catal. A: Chem.*, 2002, vol. 186, p. 89.
60. Botto, I.L., Cabello, C.I., and Thomas, H.J., *Mater. Chem. Phys.,* 1997, vol. 47, p. 37.
61. Cabello, C.I., Botto, I.L., and Thomas, J.H., *Appl. Catal., A*, 2000, vol. 197, p. 79.
62. Pettiti, I., Botto, I.L., Cabello, C.I., Colonna, S., Faticanti, M., Minelli, G., Porta, P., and Thomas, H.J., *Appl. Catal., A*, 2001, vol. 220, p. 113.
63. Mazurelle, J., Lamonier, C., Lancelot, C., Payen, E., Pichon, Ch., and Guillaume, D., *4th Int. Symp. on Molecular Aspects of Catalysis by Sulfides*, Doorn, The Netherlands, 2007, p. 17.
64. Mazurelle, J., Lamonier, C., Payen, E., and Guillaume, D., *Catal. Today*, 2008, vol. 130, p. 41.

65. Lamonier, C., Martin, C., Mazurelle, J., Harlé, V., Guillaume, D., and Payen, E., *Appl. Catal., B*, 2007, vol. 70, p. 548.

66. Nikitina, E.N., *Geteropolisoedineniya* (Polyoxometalates), Moscow: Goskhimizdat, 1962.

67. Stepin, B.D., Gorshtein, I.G., Blyum, G.E., Kurdyumov, G.M., and Ogloblina, I.P., *Metody polucheniya osobo chistykh neorganicheskikh veshchestv* (Methods of Obtaining Special-Purity Inorganic Compounds), Leningrad: Khimiya, 1969.

68. *Handbuch der preparativen anorganischen Chemie*, von Brauer, G., Ed., Stuttgart: Ferdinand Enke, 1981.

69. Klyuchnikov, N.G., *Rukovodstvo po neorganicheskomu sintezu* (Guide to Inorganic Synthesis), Moscow: Khimiya, 1965.

70. Fomichev, Yu.V. and Vlasov, V.G., *Khimiya i tekhnologiya uglerodnykh materialov* (Carbon Materials: Chemistry and Technology), Samara: Samar. Gos. Tekh. Univ., 1993.

71. Siryuk, A.G. and Zimina, K.I., *Khim. Tekhnol. Topl. Masel*, 1963, vol. 2, p. 52.

72. Muijsers, J.C., Weber, Th., van Hardeveld, V., Zandbergen, H.W., and Niemantsverdriet, J.W., *J. Catal.*, 1995, vol. 157, p. 698.

73. Weber, Th., Muijsers, J.C., van Wolput, J.H.M.C., Verhagen, C.P.J., and Niemantsverdriet, J.W., *J. Phys. Chem.*, 1996, vol. 100, p. 14144.

74. Bouwens, S.M.A.M., van Veen, J.A.R., Koningsberger, D.C., de Beer, V.H.J., and Prins, R., *J. Phys. Chem.*, 1991, vol. 95, p. 123.

75. Gandubert, A.D., Krebs, E., Legens, C., Costa, D., Guillaume, D., and Raybaud, P., *Catal. Today,* 2008, vol. 130, p. 149.

76. Saih, Y. and Segawa, K., *Appl. Catal., A*, 2009, vol. 353, p. 258.

77. Alstrup, I., Chorkendorff, I., Candia, R., Clausen, B.S., and Topsøe, H., *J. Catal.*, 1982, vol. 77, p. 397.

78. Frizi, N., Blanchard, P., Payen, E., Baranek, P., Lancelot, C., Rebeilleau, M., Dupuy, C., and Dath, J.P., *Catal. Today*, 2008, vol. 130, p. 32.

79. Koranyi, T.I., Manninger, I., Paal, Z., Marks, O., and Gunter, J.R., *J. Catal.*, 1989, vol. 116, p. 422.

80. De Jong, A.M., de Beer, V.H.J., (San), Rob van Veen, J.A., and Niemantsverdriet, J.W. (Hans), *J. Phys. Chem.*, 1996, vol. 100, p. 17722.

81. Guichard, B., Roy-Auberger, M., Devers, E., Pichon, C., and Legens, C., *Appl. Catal., A*, 2009, vol. 367, p. 9.

82. Li, M., Li, H., Jiang, F., Chu, Y., and Nie, H., *Catal. Today*, 2010, vol. 149, p. 35.